Proceedings of the Institute of Acoustics

COMPARISON OF STRING VIBRATION SPECTRA EXCITED BY DIFFERENT PIANO HAMMERS

A Stulov

Institute of Cybernetics, Tallinn, Estonia

1. INTRODUCTION

The process of string excitation by striking with a piano hammer is a very important problem of the sound formation by a musical instrument. The last preceding papers in this series [1-6] have considered several aspects of the piano hammer-string interaction. The following types of hammers were investigated: hard, soft, linear and with a force-compression characteristic approximated by a power-law dependence. To obtain better agreement with the measured data such as time histories and string spectra, various models of the string were examined. The interaction of the nonlinear hammer with the damped stiff string is described in [5,6]. This rather complicated model gives a good agreement between real and simulated string waveforms and spectra.

According to the hammer models considered before the loading and unloading of the hammer felt are the same. But the data obtained experimentally by Yanagisawa and Nakamura [7,8] show that force-compression characteristics of the hammer felt are essentially nonlinear; the slope of the dynamic force-compression characteristics is strongly dependent on the velocity of the hammer; the relationships of dynamic force versus felt deformation show the significant influence of hysteresis characteristics, so the loading and unloading of the felt are not alike. An attempt to construct the hysteretic model of the hammer-string interaction was made in [9]. However the nonanalytical model of the hammer presented there can not explain all the dynamical features of the real piano hammers.

The analytical model of the nonlinear hysteretic hammer which takes into account all the important dynamical features of the piano hammer-string interaction was developed in [10]. According to this model the felt material of the real and commonly used piano hammers possesses history – dependent properties. This models makes predictions in good agreement with experimental data [7,8] for various types of piano hammers and for a broad range of hammer velocities.

The flexible string vibration spectra excited by the different piano hammers will be analyzed here. Two types of the strongly nonlinear hammers were used for comparison. For the first hammer the force-compression characteristics is determined by the power-law dependence. The second nonlinear model [10] of the hammer takes also into account the hysteresis-type of the force-compression characteristics of the felt deformation. It will be shown that the hysteretic model of the hammer is more successful in accounting for measured string spectra than the nonlinear model used earlier. Besides, it gives a good agreement between data and predictions for any hammer velocities for a constant value of the hammer stiffness and without allowing for additional physical properties of string such as damping and stiffness.

2 HYSTERETIC HAMMER MODEL

According to this model the real piano hammer possesses history-dependent properties or just, in other words, is made of the material with memory. In this case two hereditary parameters ε and τ_0 are involved to describe the hysteretic behaviour of the hammer. The governing equation connecting the nonlinear force $F(u)$ exerted by the hammer and the felt compression $u(t)$ for hysteretic (or hereditary) hammer is presented in [10] in the form

$$F(u(t)) = F_0 \left[u^p(t) - \frac{\varepsilon}{\tau_0} \int_0^t u^p(\xi)\, exp\left(\frac{\xi - t}{\tau_0}\right) d\xi \right]. \quad (1)$$

The constant coefficient F_0 (with units such as N/mm^p) is the instantaneous hammer stiffness. The suitable values of F_0 and hereditary constants ε, τ_0 for various hammers were obtained by numerical simulation of the experiments [7,8] and are presented in [10].

The dynamic measurements of the hammers presented in [3] show that the form of the force-time curve has a symmetrical shape. Therefore, in the authors opinion, it indicates only a very minor role for dissipative forces in the hammer. We think it is not the case.

Based on the hysteretic model, the results of the numerical simulation of the experiments [7,8] are displayed in Fig.1.

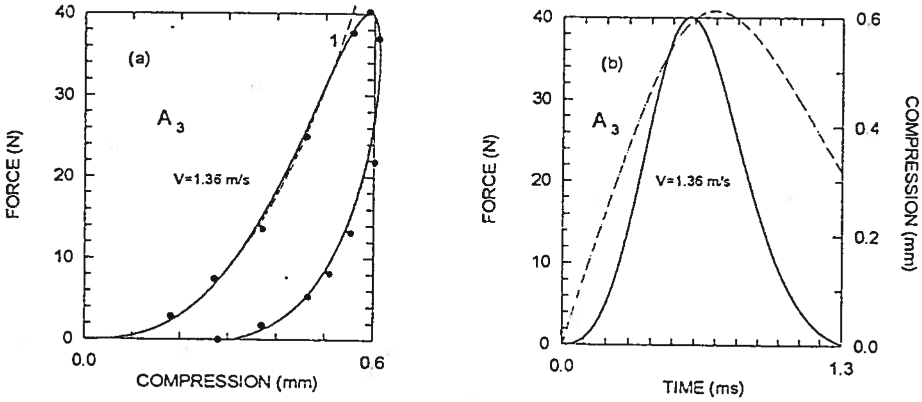

Fig.1. Dynamical features of hysteretic hammer. (a) Solid circles denote the experimental data points (Ref. 7); solid line is the simulated force-compression characteristic for medium hammer, identical to Fig.1(b) in Ref.10; dashed line 1 is approximation of the loading part of the hysteretic curve ($F_0 = 175 N/mm^p, p = 2.5$). (b) Force-time (solid line) and compression-time (dashed line) characteristics of the same hammer.

It is obvious, if even the force-time curve is very symmetrical, the force-compression curve shows the significant influence of hysteresis characteristics. Thus, the form of the force-time curve can not indicate the absence of hysteresis.

3. HAMMER-STRING INTERACTION

Consider a model of the flexible string. Similar to [4], we have the nonlinear system of equations describing the hammer-string interaction

$$\frac{dz}{dt} = -\frac{2T}{cm} g(t) + V, \quad (2)$$

$$\frac{dg}{dt} = \frac{cF_0}{2T}\left(u^p(t) - \frac{\varepsilon}{\tau_0}\int_0^t u^p(\xi)\,exp\left(\frac{\xi - t}{\tau_0}\right)d\xi\right), \tag{3}$$

$c = \sqrt{T/\mu}$, and outgoing wave $g(t)$ created by hammer-string interaction. Here, T is the string tension, μ is the linear density of the string, m and $z(t)$ are the mass and displacement of the hammer, respectively, and $u(t) = z(t) - y(0,t)$. Function $y(0,t)$ describes the string deflection at the contact point and is given by

$$\begin{aligned} y(0,t) &= g(t) + 2\sum_{i=1}^{\infty} g\left(t - \frac{2iL}{c}\right) \\ &- \sum_{i=0}^{\infty} g\left(t - \frac{2iL}{c} - \frac{2\alpha L}{c}\right) + \sum_{i=0}^{\infty} g\left(t - \frac{2iL}{c} - \frac{2\beta L}{c}\right). \end{aligned}$$

It is assumed that the string of length L extends from $-\beta L$ to αL with $\beta = 1 - \alpha$. The initial conditions at $t = 0$, the moment when the hammer first contacts the string, are taken to be $g(0) = z(0) = 0$, and $dz(0)/dt = V$, the initial hammer speed. The system of Eqs. (2), (3) was solved numerically by a modified Euler's method. In case of $\varepsilon = 0$ we have the interaction of the usual nonhysteretic hammer with a flexible string. The comparison of this nonhysteretic hammer model with the second model describing the interaction of the hereditary hammer ($\varepsilon > 0$) with a flexible string is presented below.

4. CALCULATION OF MODE ENERGY SPECTRUM

It is naturally of great interest to predict also the spectra of the string motion. The simple method is the calculation of the mode energy spectrum directly from the force history. The general expression for the string mode energy is

$$E_n = \frac{M\omega_n^2}{4}(A_n^2 + B_n^2). \tag{4}$$

where

$$A_n = \frac{2\,sin(\alpha n\pi)}{n\pi c\mu}\int_0^{t_0} F(s)\,cos(\omega_n s)\,ds, \quad B_n = \frac{2\,sin(\alpha n\pi)}{n\pi c\mu}\int_0^{t_0} F(s)\,sin(\omega_n s)\,ds. \tag{5}$$

The mode energy level is determined by $EL_n = 10\,log(E_n/E_0)$. Here $M = \mu L$ is the total string mass; $\omega_n = nc\pi/L = n\omega_0$ is the string mode angular frequency; t_0 is the contact time; $E_0 = mV^2/2$ is the initial energy of the hammer. A few of the spectra found in this way will be shown in the following section.

5. SPECTRA COMPARISON

We should like to know whether the hysteretic model is more successful in accounting for measured string spectra than the earlier nonlinear nonhysteretic model. Fig.2 presents comparison for the midrange note C_4. The reference level in all spectra is arbitrary for comparison with the measured data. Figure 2(a) simply repeats Fig.3 from Ref.4. For this note, the mass ratio is $m/M = 0.75$ and the fractional striking point parameter for experimentally measured data is $\alpha = (82mm)/(620mm) = 0.132$. As mentioned in [3,4], the predicted spectra for this value of α, however, lack the observed dip at $n = 8$, and therefore, to obtain the better fit the simulated spectrum was calculated for the value of $\alpha = (79.05mm)/(620mm) = 0.1275$.

This difference is explained in [3] with the inward shift of nodes for clamped ends of a stiff string. We can not agree with this explanation. If the stiffness of the string is taken into account, we must calculate the spectrum for the stiff string. The difference between the spectra of the stiff and flexible string is more essential. In our opinion, the hysteretic model of the hammer gives the possibility to simulate the measured spectra without using the complicated models of string such as a stiff string, or a string with damping .

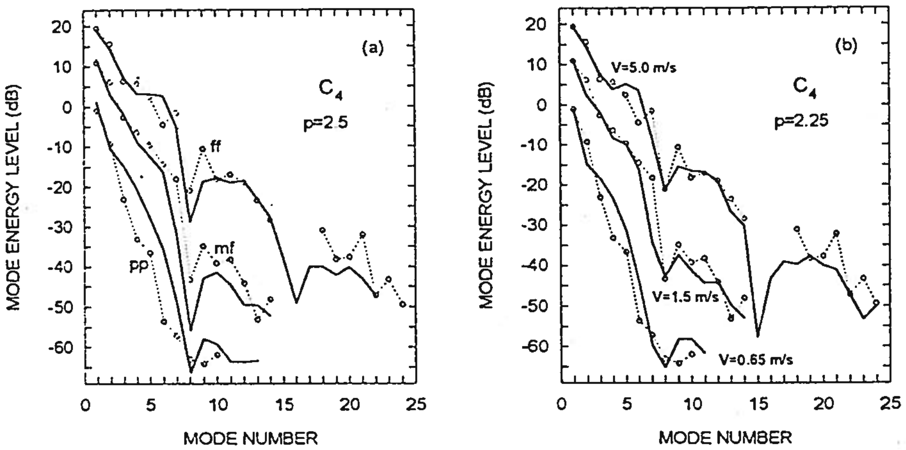

Fig.2. Spectra for middle C_4 ($f = 262Hz, L = 620mm, M = 11.8g$). (a) Measured at three different dynamic levels (light circles); predicted with nonlinear nonhysteretic ($\varepsilon = 0$) model (solid lines), using $m/M = 0.75, \alpha = 0.1275, p = 2.5$, and three values for hammer compliance; identical to Fig.3 (a,b) in Ref.4. (b) The same measured data, as in (a) (light circles); predicted with hysteretic model ($\varepsilon = 0.955, \tau_0 = 10\mu s$) (solid lines), using $m/M = 0.75, \alpha = 0.132, p = 2.25, F_0 = 200N/mm^p$, for the various hammer velocities.

This fact illustrates Fig.2(b). Using the hysteretic hammer model, the flexible string vibration spectra were simulated to obtain the agreement with measured data. The agreement between predictions and data, while not perfect, is better, than gives the nonhysteretic model. Besides, the observed dip at $n = 8$ is obtained by using $\alpha = 0.132$, or for the same value, as in the experiment.

The simulated spectra in Fig.2(a) were calculated in [4] for nondimensional values of the hammer compliance coefficients C. In nondimensional variables used there, the value $C^{-1}V^{p-1}$ is constant for each predicted spectrum. Thus, the each curve in Fig.2(a) may be interpreted as calculated for the different hammer velocities and corresponding compliances.

The simulated spectra presented in [4] and in Fig.2(a) were recalculated by our computer program in dimensional variables. In fact, in Fig.2(a) our results are presented for nonhystretic ($\varepsilon = 0$)

model, that are the same, as in Fig.3(b) in Ref.4. Thus, we had proved, if the initial hammer velocity is equal to $V = 5m/s$ (ff), then the dimensional value of the hammer stiffness constant is equal to $F_0 = C^{-1} = 7.75N/mm^{2.5}$ in our quotation. Taking into account the constant value of the stiffness constant for each hammer (this is the hammer parameter) and for any hammer velocity, for mf level we have $V = 1.74m/s$, and for pp level $V = 1.2m/s$. This follows from the presented in [4] predicted spectra calculated by using nonhysteretic nonlinear hammer model. However, these values of hammer velocity do not correspond to the musical levels mf and pp.

Of course, we may choose the right values of the hammer velocities for these levels, for example $V = 1.5m/s$ for mf and $V = 0.65m/s$ for pp, but in this case the values of the hammer stiffness would be completely different ($F_0 = 9.7N/mm^{2.5}$ and $F_0 = 19.1N/mm^{2.5}$, respectively). Therefore, the hammer stiffness is not a constant in nonhysteretic model, and we must change this value for various hammer velocity.

It is clear, that the nonhysteretic model can not explain the experimentally measured spectra for the real values of the hammer parameters. The results presented in Fig.2(b) based on the hysteretic hammer model describe the measured data quite well, and for the hammer stiffness F_0, that is a constant value for each hammer velocity.

6. TIME-DOMAIN SIMULATIONS

The spectra presented in Fig.2 are calculated by using the different models. However, they are very similar for the choosing values of hammer's parameters. We should like to know what is the difference between these hammers if we consider the hammer - string interaction in time-domain. In Fig.3 the results of the hammer - string interaction corresponding to the spectra in Fig.2 are

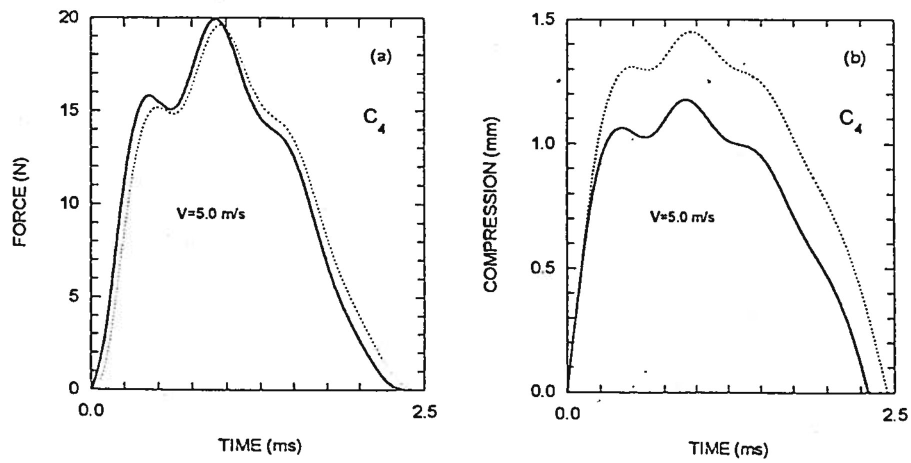

Fig.3. Interaction of hammers with initial velocity $V = 5.0m/s$ with a flexible string, using the same hammer's parameters, as in Fig.2. (a) Force histories. (b) Compression histories; for hysteretic (solid line) and nonhysteretic (dotted line) hammers.

presented in the form of force and compression histories. For the initial hammer velocity $V = 5m/s$ the force-time curves are very similar (in the same way as spectra, see Fig.2). The maximum compression of hysteretic hammer is significantly less than the compression of nonhysteretic one, but the both are larger than the string diameter ($d = 1.025mm$). It indicates that the chosen hammer is too soft.

The dynamical features of these hammers are presented in Fig.4. The numerical simulation of the interaction of hammers with a fixed target (as in [10]) permits to compare their force-compression characteristics. The loading and unloading of the nonhysteretic hammer are alike (along the curves 1 and 2). In reality, curve 1 is extended up to $F_{max} = 11.1N$. The force-compression characteristics of the nonhysteretic hammers are very different for each velocity, and curves 1 and 2 are inconsistent with the loading part of hysteretic curves. The process of interaction of the hammer with a target for $V = 1.5m/s$ is more prolonged in time and the hammer compression is less for hysteretic hammer, than for nonhysteretic one. Nevertheless, the both hammers create the almost resembling spectra.

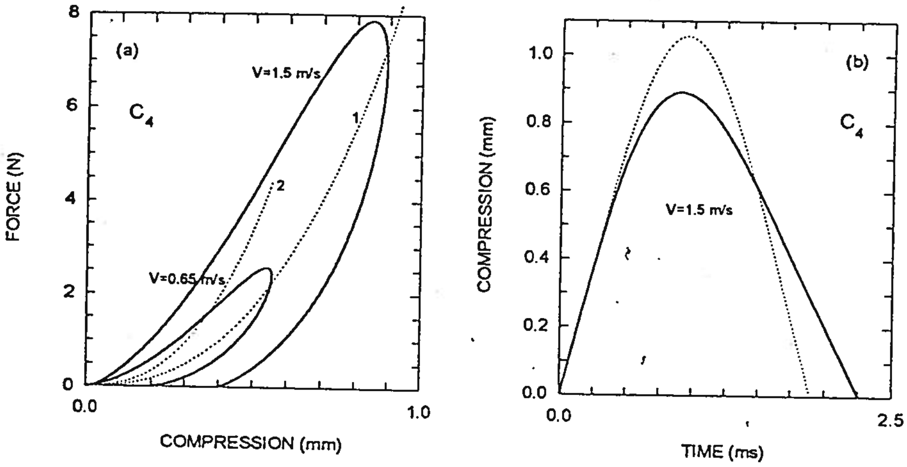

Fig.4.Two hammers comparison. (a) Dynamical force-compression characteristics of hammers simulated at two different velocities; solid lines for hysteretic hammer using $\varepsilon = 0.955, \tau_0 = 10\mu s, p = 2.25, F_0 = 200N/mm^p$; dotted lines for nonhysteretic hammer; line 1 using $p = 2.5, F_0 = 9.7N/mm^p, V = 1.5m/s$; line 2 using $p = 2.5, F_0 = 19.1N/mm^p, V = 0.65m/s$. (b) Compression histories corresponding to $V = 1.5m/s$ from (a); for hysteretic (solid line) and nonhysteretic (dotted line) hammers.

For this velocity the maximum value of compression of nonhysteretic hammer is equal to $1.055mm$. This value is greater than the string diameter. Therefore, to avoid mistakes, the dynamical measurements for this hammer must be made for velocities less than $1.3m/s$. Thus the nonhysteretic model can predict the measured spectra but gives too large values of the hammer compression.

We may also compare the hysteretic and nonhysteretic hammers in other way. Suppose, we have the measured hysteretic force-compression characteristic, for example shown in Fig.1(a). By numerical simulation of these data, we had obtain in [10] the values of all hysteretic hammer's parameters. We have the approximation of the loading part of the measured force-compression characteristic (curve 1 in Fig.1(a)), also. Thus, we may consider the interaction of these two hammers with a flexible string and predict the force histories and excited spectra. Fig.5 shows the difference between these hammers in time and frequency - domain.

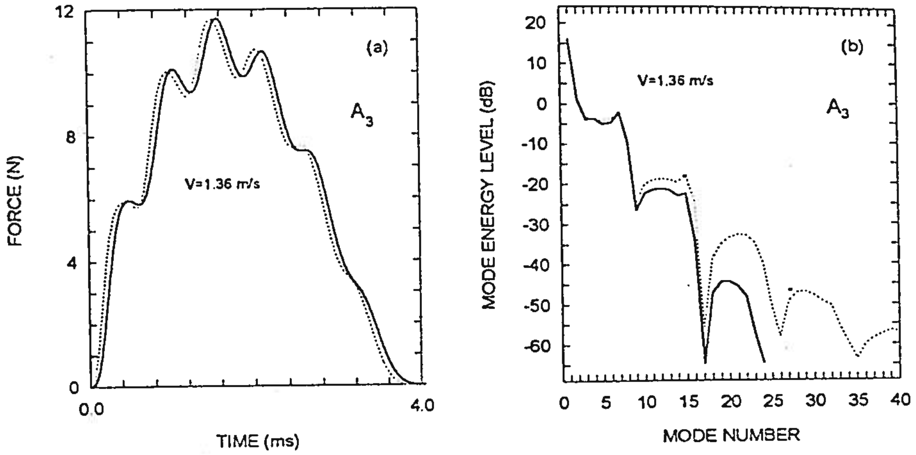

Fig.5. Force histories (a), and spectra envelopes (b) for nonlinear medium hammer A_3 and flexible string with parameters presented in Ref.10. Solid lines represent the results for hysteretic hammer, using $\varepsilon = 0.956, \tau_0 = 7\mu s, p = 3.3, F_0 = 3580 N/mm^p$, dotted lines for nonhysteretic hammer, using $F_0 = 175 N/mm^p, p = 2.5$

The force-time histories of two types of hammers almost coincide, in spite of the huge difference of hammer's parameters, but in frequency - domain the spectrum of the string vibrations excited by a hysteretic hammer is much shorter. Furthermore, the spectral slope for the hysteretic hammer is approximately 1.5 times steeper than for the nonhysteretic hammer.

7. SUMMARY

The analysis of the results obtained shows that the nonlinear hysteretic model of the hammer provides predictions about the vibration spectra of struck strings for real pianos that come closer to measured data than predicts the nonhysteretic model. In addition to the correct spectra, the hysteretic model gives more suitable values of the hammer compression.

The harmonics attenuation for flexible string excited by a nonhysteretic hammer is rather small at all. On the contrary, the number of harmonics excited in a real grand piano string is not so high. To obtain the steeper spectral slope, some more complicated models of the string with a stiff and damping terms were used in [5,6] for numerical simulation of the experiments. The hysteretic hammer model includes the absorption within a hammer material and may explain the real piano spectra without any additional damping in string.

The hysteretic model may predict the excited spectra for the various hammer velocity using only one value of the hammer stiffness, that is the hammer parameter indeed.

Figures 2 and 4 show, and we must repeat here once again, that if the hammer stiffness C and stiffness nonlinearity exponent p are defined from the static measurements, or for some certain hammer velocity, these values can not give the true description of the hammer-string interaction for the other velocities of hammer in case of using the nonhysteretic hammer model.

In fact, many various researchers are trying to describe the process of the hammer-string interaction with the aid of the nonlinear nonhysteretic model using the measured data which were experimentally obtained for the different hammers with the arbitrary initial velocities. Thus, for the each experiment the new different values of the hammer compliance C and stiffness nonlinear exponent p were find. No wonder that no definite trends of p and C are discovered.

Unfortunately, we have not the opportunity to carry on the own experiments. However, the numerical simulations using the hysteretic hammer model may give the possibility to find the dependence of the values of hammer's parameters on a key number. It seems, the values of the hereditary parameters ε and τ_0 have a certain trend from bass to treble. So, definitely, ε increases and τ_0 decreases with a key number. The hammer stiffness is a constant value in hysteretic model. This parameter depends on the hammer size, wear, manufacturers. For the one certain set of piano hammers it is possible to find the values of the instantaneous hammer stiffness F_0. In our opinion, for the one set of hammers the value of p increases also with a key number.

8. REFERENCES

[1] D.E. Hall, 'Piano string excitation II: General solution for a hard narrow hammer', J. Acoust. Soc. Am. 81 p535 (1987).

[2] D.E. Hall, 'Piano string excitation III: General solution for a soft narrow hammer', J. Acoust. Soc. Am. 81 p547 (1987).

[3] D.E. Hall and A. Askenfelt, 'Piano string excitation V: Spectra for real hammers and strings', J. Acoust. Soc. Am. 83 p1627 (1988).

[4] D.E. Hall, 'Piano string excitation VI: Nonlinear modeling', J. Acoust. Soc. Am. 92 p95 (1992).

[5] A. Chaigne and A. Askenfelt, 'Numerical simulation of piano strings. I. A physical model for a struck string using finite difference methods', J. Acoust. Soc. Am. 95 p1112 (1994).

[6] A. Chaigne and A. Askenfelt, 'Numerical simulation of piano strings. II. Comparisons with measurements and systematic exploration of some hammer-string parameters', J. Acoust. Soc. Am. 95 p1631 (1994).

[7] T. Yanagisawa and K. Nakamura, 'Dynamic compression characteristics of piano hammer', Trans. of Musical Acoust. Technical Group Meeting of Acoust. Soc. Jpn. 1 p14 (1982).

[8] T. Yanagisawa and K. Nakamura, 'Dynamic compression characteristics of piano hammer felt', J. Acoust. Soc. Jpn. 40 p725 (1984).

[9] X. Boutillon, 'Model for piano hammers: Experimental determination and digital simulation', J. Acoust. Soc. Am. 83 p746 (1988).

[10] A. Stulov, 'Hysteretic model of the grand piano hammer felt', J. Acoust. Soc. Am. 97 p2577 (1995).

Proceedings

Institute of Acoustics

ISMA'97

Vol. 19: Part 5 (1997)
Book 1: (pp1 – 250)
ISMA '97 Conference